

Spin-Lattice Relaxation of Water in Cement Gels

R. Blinc, J. Dolinšek, G. Lahajnar, A. Sepe, I. Župančič, and S. Žumer
J. Stefan Institute, E. Kardelj University, Ljubljana, Yugoslavia

F. Milia

Nuclear Research Center Demokritos, Athens, Greece

M. M. Pintar

Waterloo NMR Center, Department of Physics, University of Waterloo, Waterloo, Ontario, Canada

Z. Naturforsch. **43 a**, 1026–1038 (1988); received July 31, 1988

The time evolution of the magnetization relaxation recovery of exchangeable water in ordinary Portland cement and white cement have been studied as functions of the hydration time together with the temperature and Larmor frequency dependence of the proton spin-lattice relaxation rates. The water self-diffusion coefficient was also studied as a function of both the hydration time and the diffusion time. The results show that the exchangeable water relaxes via cross relaxation to the gel protons, which are in turn relaxed via spin diffusion to paramagnetic impurities. The roughness of the gel-water interface and the wide distribution of pore sizes result in a stretched exponential nuclear magnetization relaxation recovery with the exponent reflecting the fractal geometry of the hydrating cement gel.

Key words: NMR, cement gels, hydration.

I. Introduction

The interaction of water with the surface in a porous solid is of interest in a wide range of applications. It has been generally found that the fluid in a porous solid has a faster nuclear spin-lattice relaxation rate than the corresponding bulk fluid. This relaxation rate enhancement depends on the ratio between the pore surface area and the pore volume. The above effect has been recently used to study the hydration of cement [1–7].

Ordinary Portland cement (OPC) powder contains [1] four main components: tricalcium silicate (C_3S), β -dicalcium silicate (β - C_2S), tricalcium aluminate (C_3A) and a ferrite solid solution (C_4AF). The initial reaction with water produces a surface layer of hydration products – mainly amorphous calcium silicate hydrate (CSH) gel – around each grain. With further reaction the hydration product coatings extend and meet each other so that the CSH gel and some newly formed calcium hydroxide crystals fill out most of the space between the grains [1]. Whereas the rate determining step in the early stages of hydration is a chemical reaction (such as the reaction between the

silicates and water), ion diffusion through the gel becomes the slowest step and thus controls the speed of solidification as soon as the gel coating becomes thick enough [2]. The gel is more densely packed in some regions than in others so that pores, containing a saturated water solution of calcium hydroxide, are formed [1–2]. Transmission electron micrographs indicate [2] that the porous structure of the gel is very open and has the appearance of self-similarity [3].

It has been recently shown [4] by small angle neutron scattering that the porous structure of cement gels is indeed self-similar at long enough hydration times and seems to become after 28 days of hydration [4] a fractal object with a surface fractal dimension of $D_s \approx 2.8$. The time evolution of the fractal geometry has been followed by nuclear magnetization relaxation recovery measurements [5]. The proton magnetization recovery of exchangeable water in cement pastes changes from a simple exponential form ($\alpha = 1$) found in the “dormant” period to a “stretched” exponential form

$$M(t) = M_0(1 - e^{-(t/T_1)^\alpha}), \quad (1)$$

in later stages of the hydration process [5]. Expression (1) means that we deal with a distribution of spin-lattice relaxation rates $P(T_1^{-1})$ which is related to the

Reprint requests to R. Blinc, J. Stefan Institute, 61111 Ljubljana, Jamova 39, Yugoslavia.

0932-0784 / 88 / 1200-1026 \$ 01.30/0. – Please order a reprint rather than making your own copy.



Dieses Werk wurde im Jahr 2013 vom Verlag Zeitschrift für Naturforschung in Zusammenarbeit mit der Max-Planck-Gesellschaft zur Förderung der Wissenschaften e.V. digitalisiert und unter folgender Lizenz veröffentlicht: Creative Commons Namensnennung-Keine Bearbeitung 3.0 Deutschland Lizenz.

Zum 01.01.2015 ist eine Anpassung der Lizenzbedingungen (Entfall der Creative Commons Lizenzbedingung „Keine Bearbeitung“) beabsichtigt, um eine Nachnutzung auch im Rahmen zukünftiger wissenschaftlicher Nutzungsformen zu ermöglichen.

This work has been digitalized and published in 2013 by Verlag Zeitschrift für Naturforschung in cooperation with the Max Planck Society for the Advancement of Science under a Creative Commons Attribution-NoDerivs 3.0 Germany License.

On 01.01.2015 it is planned to change the License Conditions (the removal of the Creative Commons License condition “no derivative works”). This is to allow reuse in the area of future scientific usage.

pore size distribution. The proton spin-lattice relaxation rate T_1^{-1} of “exchangeable” water reflects [6, 7] the evolution of the specific surface of hardening cement pastes. The detailed nature of this effect is, however, still not very well understood.

In order to check on the nature of the spin-lattice relaxation mechanisms of exchangeable water in cement gels we decided to study the proton spin-lattice relaxation rate and recovery function of exchangeable water in cement gels as a function of the hydration time, temperature and proton Larmor frequency. The temperature and Larmor frequency dependences were studied after the dormant [1] period. We investigated “white” cement, where the concentration of paramagnetic Fe_2O_3 ions is smaller than in OPC. We compared the obtained results with those found for OPC and for C_3S , where there are no aluminium nuclei. In order to check on the possible fractal nature of water self-diffusion in cement gels [8, 9] we as well measured the water self-diffusion coefficient by pulsed field gradient (PFG) NMR as a function of both the diffusion time and the hydration time at room temperature.

II. Experimental

All experiments were performed with samples sealed in glass tubes so that the water/cement ratio did not change during the measurements. The concentration of metal ions was checked by flame spectroscopy and electron paramagnetic resonance. The analysis showed that the OPC samples contained up to one weight percent of Fe for a water/cement ratio (w/c) of 0.45, the “white cement” samples contained more than ten times less iron, i.e. about 850 micrograms of Fe per one gram of cement paste, whereas the C_3S samples contained only 63 micrograms of Fe per gram of paste. The concentration of Mn, Ni, Co and Cu ions was found to be small as compared to the iron concentration.

The spin-lattice relaxation times T_1 have been measured by the $90^\circ - \tau - 90^\circ$ method, whereas the spin-spin relaxation times T_2 have been determined by the Carr-Purcell $90 - 180 - \text{echo} - 180 - \text{echo} \dots$ techniques with the time interval between the pulses exceeding $100 \mu\text{s}$. The self-diffusion coefficients were obtained by the pulsed field gradient NMR spin echo [10] technique using the 90° -gradient pulse– 180° -gradient pulse–echo sequence.

III. Proton Magnetization Recovery of Exchangeable Water in Cement and the Distribution of Pore Sizes

Since the exchange between “free” water molecules and the ones “bonded” to the gel surface is generally fast within a given micropore, whereas the exchange of water between different micropores is generally slow [5–7] in the advanced stages of cement hydration, we have in cement a distribution of T_1^{-1} values $P(T_1^{-1})$ reflecting the pore size distribution $g(\xi)$ and geometry.

The complete proton magnetization recovery thus represents a weighted average of recovery functions over the various pores:

$$R(t) = \frac{M_0 - M(t)}{M_0} = \int P(T_1^{-1}) \exp(-t/T_1) d(T_1^{-1}), \quad (2)$$

where

$$P(T_1^{-1}) d(T_1^{-1}) = g(\xi) d\xi. \quad (3)$$

In such a case the magnetization recovery function $R(t)$ is the Laplace transform of the relaxation rate distribution function $P(T_1^{-1})$, which is related to the pore size distribution function $g(\xi)$. Here ξ is a characteristic (dimensionless) pore size.

The extraction of $P(T_1^{-1})$ and $g(\xi)$ from the above Fredholm integral equation of the first kind (2) is possible if the experimental magnetization recovery is precisely recorded in a broad time interval [11].

There is no quantitative microscopic theory of the hydration of cement – and the time development of $g(\xi)$ – as yet.

If we, for example, consider the solidification of cement as a connectivity [9] transition between a zero dimensional network (the initial water dispersion of cement grains) and the three dimensional network in the fully hydrated cement, we find from percolation theory [9] the pore size distribution $g(\xi)$ close to the percolation threshold to be given by

$$g(\xi) = A \exp(-C \xi^y). \quad (4)$$

The pore surface to volume ratio (i.e. fraction of the bonded water) is within the same model similarly described by the scaling law

$$\eta(\xi) = \eta_0 \xi^{-x}, \quad (5)$$

where η_0 is proportional to the active internal surface of cement and $x = D_v - D_s$ stands for the difference between the volume and surface fractal dimensionalities.

For the case that $T_1^{-1} \approx T_{1b}^{-1} \eta(\xi)$ – see Chapt. III – one finds from (2)

$$R(t) = \int_0^\infty A e^{-C\xi^y} e^{-(t/T_{1b})\eta(\xi)} d\xi, \quad (6)$$

leading for long enough times asymptotically to a stretched exponential magnetization recovery

$$R(t) \propto \exp[-(t/\tilde{T}_1)^\alpha], \quad (7)$$

where the time constant

$$\frac{1}{\tilde{T}_1} = \frac{1}{(T_{1b})} \eta_0 2^\alpha C^{(x/y)} \quad (8)$$

is proportional to their active internal surface of cement and the effective relaxation rate of water molecules bonded to the surface (T_{1b}^{-1}). Here

$$\alpha = y/(x+y). \quad (9)$$

In the following we shall – for simplicity – use T_1 instead of \tilde{T}_1 even though the spin-lattice relaxation time was determined via (7). In the spin-lattice relaxation experiment based on the free induction decay one can, by varying the time delay of the observation point (δ), study the partial magnetization recovery. For $\delta \rightarrow 0$ complete recovery is registered, while for $\delta > 0$ only contributions of pores where $T_2^* > \delta$ are important. So the lower limit of the integral in (6) must be substituted with ξ_δ corresponding to $\eta(T_2^* = \delta)$, see (5). The relation between T_2 and η will be discussed in the next chapter. The recovery can be here no more described by a simple stretched exponential form (7). In the limit $\delta \rightarrow \infty$ it becomes mono-exponential.

IV. Relaxation Mechanisms of Exchangeable Water in Cement Gels

According to Seligman [1] there are four types of water in saturated cement pastes: free water, physically adsorbed water, interlayer and pore water, and chemically bonded water such as in $\text{Ca}(\text{OH})_2$. The apparent spin-spin relaxation time T_2^* (determined from the free induction decay and thus affected by sample heterogeneity etc.) of free water [6] is about 1 s, the T_2^* of physically adsorbed water ≈ 1 ms, T_2^* of micropore and interlayer “exchangeable” water between 20 and 90 μs and T_2^* of $\text{Ca}(\text{OH})_2$ of the order of 10 μs . The T_2^* of cement gel is of the same order of magnitude as that of micropore water ≈ 20 –70 μs , indicating fast exchange processes. The spin-lattice

relaxation time [6] of solid $\text{Ca}(\text{OH})_2$ is of the order of 500 ms, whereas the T_1 of the micropore water and solid gel is much shorter and approaches 1 ms for T_2 values larger than 40 μs after long enough hydration times (Figure 1).

The most striking characteristic of the spin-lattice relaxation rate T_1^{-1} of “exchangeable” water (i.e. interlayer, micropore and gel adsorbed component) is that it is proportional [7] to the specific surface and compressive and bending strengths of hardening cement pastes (Figure 2). This demonstrates that the relaxation is indeed surface induced.

The exchange between bonded and free water molecules in a given pore is determined by two hierarchical processes: first a molecule has to diffuse from the bulk to the surface, and then it must exchange with a molecule bonded to the surface. Therefore the probability for a bulk molecule to exchange with a surface-bonded molecule is given by a product of two independent probabilities, namely: (i) w_1 – the probability to be in the surface layer where the exchange can take place, and (ii) w_2 – the probability to undergo the exchange.

If τ_b is the residence time of a given “bonded” molecule on the surface, the probability for its exchange is given by $w_2 = 1/\tau_b$.

Further, one can introduce the diffusion time

$$\tau_{\text{diff}} = L^2/6D, \quad (10)$$

which measures the time spent by a “free” water molecule to cross a typical pore dimension L . D is the water diffusion constant. For $L \approx 1000$ Å and $D \approx 10^{-6}$ cm²/s one finds $\tau_{\text{diff}} \approx 10^{-7}$ s. Since this time is short compared to the residence time $\tau_b \approx 10^{-4}$ s, the probability w_1 for a given bulk molecule to be in the surface layer ready to exchange with the surface-bonded molecule is proportional to the surface-to-volume ratio S/V , so that

$$w_1 = \eta = K \cdot S/V, \quad (11)$$

where K is the thickness of the surface layer.

In such a limit the life time of a free molecule in the bulk τ_f given by $(w_1 w_2)^{-1}$ – the inverse of the probability for a bulk molecule to exchange with a bonded one – reduces to the ratio

$$\tau_f = \tau_b/\eta. \quad (12a)$$

Therefore, in the calculation of physical properties like magnetic relaxation rate or molecular diffusion constant, time averaging can be substituted by the spatial averaging.

For a spherical pore of radius R and a water surface layer of thickness K , η is given by

$$\eta = 3K/R. \quad (12b)$$

If, for instance, we assume that the surface layer is monomolecular we get, with $K = 2 \text{ \AA}$ and $R = 1000 \text{ \AA}$, $\eta = 6 \times 10^{-3}$ and $\tau_f = 1.6 \times 10^{-2} \text{ s}$ if $\tau_b \approx 10^{-4} \text{ s}$.

As the life-time τ of a molecule in a given phase within the micropore is short compared to the spin-lattice relaxation time associated with this phase we have – within a given micropore – a unique T_1 characterizing protons in different environments:

$$\frac{1}{T_1} = \left(\frac{1}{T_{1b}} \right) \eta + \left(\frac{1}{T_{1f}} \right) (1 - \eta) \approx \left(\frac{1}{T_{1b}} \right) \eta; \quad T_{1b} \ll T_{1f}, \quad \tau_f \ll T_{1f}, \quad \tau_b \ll T_{1b} \quad (13)$$

and mono-exponential magnetization relaxation recovery:

$$R(t)_{\text{pore}} = (M_0 - M(t))/M_0 = \exp(-t/T_1), \quad t \gg \tau_f. \quad (14)$$

In view of the slow exchange of water between different micropores, the distribution of pore sizes will result in a distribution of T_1 values and a non-exponential relaxation recovery such as given by (1). The subscript “b” refers to “bonded” water molecules near the solid surface of the cement gel and “f” to “free” water molecules in the micropore. η is the fraction of “bonded” water molecules at the gel surface:

$$\eta = \frac{N_b}{N_b + N_f}, \quad (15a)$$

which is determined by the surface to volume ratio S/V of the micropores: $\eta = K \cdot S/V$.

Since $\tau_f \ll T_{1b} = 1 - 0.1 \text{ ms} \ll T_{1f} \approx 1 \text{ s}$, it is clear that the “fast” exchange approximation used in (13) and (14) is indeed valid for a wide range of pore sizes. For $\eta \ll 1$ one can – using (12b) – rewrite (13) as

$$\frac{1}{T_1} = \frac{1}{T_{1f}} + \frac{1}{T_{1b}} \cdot \eta = A + B/R. \quad (15b)$$

Expression (15b) directly shows the relation between the water relaxation rate in a given micro-pore and the pore size R . Within the same approximation one finds for the effective spin-spin relaxation rate T_2^{-1} for a given micropore:

$$\frac{1}{T_2} = \left(\frac{1}{T_{2b}} \right) \eta + \left(\frac{1}{T_{2f}} \right) (1 - \eta) \approx \left(\frac{1}{T_{2b}} \right) \eta, \quad \tau_f \ll T_{2f} \ll T_{2b}. \quad (16)$$

Since T_{2b} is much shorter than T_{1b} , the validity of the fast exchange approximation is here much more restricted than in the case of (13). At long enough hydration times one might even reach the “slow motion” limit, where we have two separate effective spin-spin relaxation rates:

$$T_{2b}^{-1} = T_{2b}^{-1} + \tau_b^{-1} \quad (17a)$$

and

$$T_{2f}^{-1} = T_{2f}^{-1} + \tau_f^{-1}. \quad (17b)$$

Whereas the validity of (13) and (16) has been checked previously, the exact nature of the spin-lattice relaxation time of water molecules bonded to the surface of the gel T_{1b} is still not well understood. Its value in OPC ($\approx 0.1 - 1 \text{ ms}$) is so short [6] that it cannot be due to simple dipolar relaxation of water molecules even if they would be moving at the optimum rate $\tau = 1/\omega_L$ for relaxation.

There are several different relaxation mechanisms which could explain the observed extremely short value of T_{1b} : a) relaxation induced by fluctuating local magnetic fields due to paramagnetic impurities, b) relaxation via magnetic dipolar coupling to quadrupolar nuclei, c) relaxation via fast diffusion in internal magnetic field gradients due to the water-cement interface, and d) cross-relaxation between the bonded water molecules and the gel, where spin diffusion to paramagnetic impurities or quadrupolar nuclei like Al ($I = 5/2$), is rate determining.

Let us now analyze these possibilities and see whether experiments can decide between them.

a) Fluctuating Local Magnetic Fields due to Paramagnetic Impurities

A rough estimate [10] for the proton spin-lattice relaxation rate induced by fluctuating local fields due to a paramagnetic impurity with a spin S at a distance r from the water molecule bonded to the gel surface is

$$\frac{1}{T_{1b}} = \frac{9}{2} \gamma_S^2 \gamma_1^2 \hbar^2 \frac{\sin^2 \vartheta \cos^2 \vartheta}{r^6} \int_{-\infty}^{+\infty} \langle S_Z(0) S_Z(t) \rangle e^{-i\omega_1 t} dt, \quad (18)$$

where $\vartheta \propto (\mathbf{H}_0, \mathbf{r})$. For

$$\langle S_Z(0) S_Z(t) \rangle = \frac{1}{3} S(S+1) \exp(-t/\tau_c)$$

one finds for a randomly oriented sample

$$T_{1b}^{-1} = C/r^6 \quad (19a)$$

with

$$C = \frac{1}{5} S(S+1) \gamma_S^2 \gamma_I^2 \hbar^2 \frac{2\tau_e}{1 + \omega_I^2 \tau_e^2}. \quad (19b)$$

For $\omega_I \tau_e \gg 1$ this yields

$$\frac{1}{T_{1b}} = \frac{2}{5} \frac{S(S+1)}{\tau_e} \left(\frac{H_e}{H_0} \right)^2, \quad (20)$$

where $H_e^2 = \frac{\gamma_S^2 \hbar^2}{r^6}$. The correlation time τ_e for the fluctuating local paramagnetic fields is here due to two different processes:

$$\frac{1}{\tau_e} = \frac{1}{\tau_s} + \frac{1}{\tau_b}. \quad (21)$$

i.e., i) electronic spin-lattice relaxation characterized by τ_s and ii) motion of the water molecule in and out of the paramagnetic field, characterized by the residence time τ_b of the water molecule at the gel surface.

It should be mentioned that this process is dominant only if most impurities (Fe^{3+}) are highly concentrated in the vicinity of the gel surface. For $\tau_e \approx 10^{-10}$ s, $r = 4$ Å, $S = 3/2$ and $H_0 = 1.5$ T one finds $T_{1b} \approx 0.05$ ms, well within the range observed in OPC. In the limit $\tau_s \ll \tau_b$ the spin-lattice relaxation rate T_{1b}^{-1} described by (20) should depend quadratically on the nuclear Larmor frequency for $\omega_L \tau_e \gg 1$. For $\tau_s \gg \tau_b$ and the case where the motion of the water molecule in and out of the paramagnetic field can be described as a time fractal process, the proton autocorrelation function is of the stretched exponential type $G(t) \propto e^{-(t/\tau)^\alpha}$ with $0 < \alpha < 1$, and one finds in the slow motion limit

$$T_1 \propto \tau^\alpha \omega_L^{(1+\alpha)}, \quad \omega_L \tau \gg 1, \quad (22a)$$

whereas in the opposite fast motion limit T_1 is frequency independent:

$$T_1 \propto \tau^{-1} \neq f(\omega_L), \quad \omega_L \tau \ll 1. \quad (22b)$$

If impurities are diluted in the solid phase (gel), their effect on bonded water protons is only indirect. Paramagnetic centres in the gel induce the relaxation of gel protons. This relaxation takes place via spin diffusion [10] from the gel protons to the paramagnetic centres and can be described by

$$\frac{1}{T_{1g}} = 4\pi N C / 3 b^3. \quad (23)$$

Here N is the number density of the paramagnetic impurities and b stands for the radius where the spin diffusion process is comparable to the direct relax-

ation. It is given by

$$b = (c/\tilde{D}_S)^{1/4}. \quad (24)$$

\tilde{D}_S is the spin diffusion coefficient, which is approximately described by

$$\tilde{D}_S \approx \frac{a^2}{30} \sqrt{M_{2H\text{gel}}}. \quad (25)$$

Here a is the inter-proton spacing in the gel and $M_{2H\text{gel}}$ is the corresponding second moment. Due to the lack of information we take for a crude estimate M_2 from data for powdered gypsum ($\text{CaSO}_4 \cdot 2\text{H}_2\text{O}$: $\sqrt{M_{2H\text{gel}}} \approx 0.3 \times 10^5 \text{ s}^{-1}$ and $a = 2.8$ Å) and combine them with the white cement data $N = 2.3 \times 10^{21} \text{ Fe}^{3+}/\text{cm}^3$, and $\tau_e \approx 10^{-10}$ s. In a field $H = 1.5$ T the resulting gel relaxation time is $T_{1g} \approx 1.2$ ms. For $\tau_e \omega_L \ll 1$, T_{1g} is frequency independent, while for $\tau_e \omega_L \gg 1$ one finds $T_{1g} \propto \omega_L^{1/2}$.

In the liquid phase, relaxation via paramagnetic impurities is for $\omega < 2D/(\text{ion size})^2 \approx 10^9 - 10^{10} \text{ s}^{-1}$ given by a simple expression:

$$\frac{1}{T_1} = \frac{16\pi^2}{15} N \gamma_S^2 \hbar^2 S(S+1) \frac{\gamma_I^2 v_w}{kT}. \quad (26)$$

Taking v_w as the viscosity of water ($\approx 10^{-3} \text{ kg/ms}$) and the same N as above one finds $T_1 = 25$ ms. In fact the concentration of paramagnetic impurities in the water cement solution in the dormant period is significantly smaller than in the cement gel in the later stages of the hydration as the cement grains are not yet dissolved.

b) Relaxation via Magnetic Dipolar Coupling to Quadrupolar Nuclei

Let us now investigate the magnetic dipolar relaxation rate of bound water molecules induced by fast fluctuations of quadrupolar (e.g. Al) nuclear spins. For this process one finds

$$T_{1H-Al}^{-1} = \frac{1}{2} M_2(H-Al) \int_{-\infty}^{+\infty} e^{i\omega t} \langle S_{ZAl}(0) S_{ZAl}(t) \rangle dt. \quad (27a)$$

Here $M_2(H-Al)$ is the proton-aluminum dipolar second moment. The autocorrelation function for the Al spin ($I = 5/2$) fluctuations can be approximated by

$$\langle S_Z(0) S_Z(t) \rangle = [S(S+1)/3] \exp[-t/T_{1Al}], \quad (27b)$$

so that

$$T_{1H-Al}^{-1} = \frac{35}{12} M_2(H-Al) T_{1Al} / [1 + \omega^2 T_{1Al}^2]. \quad (28a)$$

Since $\omega \approx 10^8 \text{ s}^{-1}$ and $T_{1\text{Al}} > 300 \mu\text{s}$, we have $\omega T_{1\text{Al}} \gg 1$, resulting in

$$T_{1\text{H-Al}}^{-1} = \frac{35}{12} M_2(\text{H-Al})/(\omega^2 T_{1\text{Al}}). \quad (28\text{b})$$

The result (28b) is analogous to the one found for paramagnetic impurities – (20) – except for the fact that the nuclear magnetic dipolar coupling is much weaker than the coupling to electronic spins. The direct contribution of fast fluctuations of the diluted Al-spins ($N_{\text{Al}} \sim 10^{21} \text{ cm}^{-3}$) to the water proton T_1 in a cement gel or on its surface is thus negligible.

For rigidly bonded water molecules there is however still another possible proton relaxation mechanism via quadrupolar nuclei, which does not exist in the case of paramagnetic impurities. In view of the random orientations of the principal axes of the Al electric field gradient tensors with respect to the external magnetic field in the cement gel, some Al and proton transition frequencies may coincide at low enough external fields. Since the proton-proton cross-relaxation rate $W_{\text{H-H}}$ is larger than the proton-Al cross-relaxation rate $W_{\text{H-Al}}$, which is in turn faster than the Al spin-lattice relaxation rate $T_{1\text{Al}}^{-1}$ (here rigid bonding is crucial), we have

$$W_{\text{H-H}} > W_{\text{H-Al}} > T_{1\text{Al}}^{-1}, \quad (29)$$

so that a common spin temperature will be established in the proton-resonant Al Zeeman reservoir. The H-Al cross-relaxation rate is effective only if the Al Zeeman perturbed quadrupole resonance or quadrupole perturbed Zeeman resonance lies within the dipolar width of the proton NMR line $\Delta\nu \approx [M_2(\text{H-H})]^{1/2} + [M_2(\text{H-Al})]^{1/2}$. Let us denote with $\Delta N(\nu)/N$ the fraction of Al-nuclei satisfying this condition at a given proton frequency ν . Since we have a common spin temperature β in the proton-resonant Al Zeeman reservoir, one finds

$$\frac{d\beta}{dt} = -\frac{1}{T_1(\nu)}(\beta - \beta_L), \quad (30)$$

where

$$\begin{aligned} \frac{1}{T_1(\nu)} &= \frac{C_{\text{Al, res}}}{C_{\text{Al, res}} + C_{\text{H}}} \frac{1}{T_{1\text{Al}}} + \frac{C_{\text{H}}}{C_{\text{Al, res}} + C_{\text{H}}} \frac{1}{T_{1\text{H}}} \\ &\approx \frac{C_{\text{Al, res}}}{C_{\text{H}}} \frac{1}{T_{1\text{Al}}} + \frac{1}{T_{1\text{H}}}, \end{aligned} \quad (31\text{a})$$

with

$$C_{\text{Al, res}} = \frac{\Delta N(\nu)}{N} C_{\text{Al}} \ll C_{\text{H}} \quad (31\text{b})$$

standing for the heat capacity of the resonant part of the Al Zeeman and quadrupolar energy reservoir. Here C_{Al} and C_{H} are the total heat capacities of the Al and H nuclei, respectively, whereas $T_1(\nu)$ is the magnetic field dependent relaxation time of the combined proton-resonant Al Zeeman reservoir, which is most conveniently measured via the abundant species, i.e. via protons.

It should be noted that the Al quadrupole coupling constant is typically of the order of a few MHz. The above mechanism is thus expected to be important at rather low proton Larmor frequencies or in the rotating frame but not at frequencies above 30 MHz.

c) Relaxation via Fast Diffusion in Internal Magnetic Field Gradients Due to the Water-Cement Interface

It is well known that the magnetic field inside an inhomogeneous medium will in general be inhomogeneous. This can be easily understood if one remembers that a magnetic dipole moment is induced in a sphere located in an otherwise uniform magnetic field \mathbf{B}_0 , provided the diamagnetic susceptibility of the sphere differs from that of the surrounding medium. The field gradient along \mathbf{B}_0 outside the sphere is proportional [11] to B_0 , the difference in the diamagnetic susceptibilities $\Delta\chi$ and the inverse of the sphere radius:

$$G_Z \approx \frac{\pi B_0 \Delta\chi}{R_0}. \quad (32)$$

Since

$$\chi_{\text{spec}}(\text{H}_2\text{O}) = -0.699 \times 10^{-6} \text{ cgs}$$

whereas

$$\chi_{\text{spec}}(\text{CaO}) = -0.27 \times 10^{-6} \text{ cgs},$$

$$\chi_{\text{spec}}(\text{SiO}_2) = -0.493 \times 10^{-6} \text{ cgs},$$

$$\chi_{\text{spec}}(\text{Al}_2\text{O}_3) = -0.098 \times 10^{-6} \text{ cgs},$$

the difference $\Delta\chi$ will be of the order of 10^{-6} in cgs units. For small enough spheres ($R_0 = 50 \text{ \AA}$) the internal gradients in a field $B_0 = 10^4$ Gauss become extremely large $G_Z = 10^5$ Gauss/cm. This should result in a field dependent inhomogeneous broadening of the free induction decay:

$$1/T_2' = KB_0 + 1/T_2. \quad (33)$$

An additional spin-lattice relaxation mechanism should also be produced if the molecules are diffusing from one region to another in the heterogeneous

sample with large internal field gradients. The additional contribution to the spin-lattice relaxation rate will be approximately given by

$$\frac{1}{T_1} \approx (\gamma_H \Delta B_Z)^2 \frac{\tau}{1 + \omega_L^2 \tau^2}, \quad (34)$$

where ΔB_Z is the change in the magnetic field along \mathbf{B}_0 produced by diffusion in the time τ . The magnitude of ΔB_Z depends on the mean square nuclear displacement in the field gradient G_Z . The interesting point is that we have here a field dependent T_1 in the fast motion regime

$$\frac{1}{T_1} \propto B_0^2 \tau, \quad \omega_L \tau \ll 1 \quad (35)$$

and *not* in the slow motion regime, where

$$\frac{1}{T_1} \propto \frac{1}{\tau}, \quad \omega_L \tau \gg 1. \quad (36)$$

This magnetic field dependence of T_1 is thus just opposite to the one usually obtained – e.g. the BPP case –, where

$$\frac{1}{T_1} \propto \frac{1}{\omega_L^2 \tau} \quad \text{for } \omega_L \tau \gg 1$$

and

$$\frac{1}{T_1} \propto \tau \quad \text{for } \omega_L \tau \ll 1.$$

d) Cross-Relaxation between the Bonded Water Molecule and the Gel

If the residence time τ_b of a water molecule at the gel surface is long as compared to the time τ_{cross} for magnetization transfer between the water molecule and the gel, cross-relaxation effects may become important. Here the rate of the magnetization exchange between bonded water molecules and gel is given by

$$\tau_{bg}^{-1} = \tau_{\text{cross}}^{-1} \approx \sqrt{M_{2H \text{ gel-surface}}}, \quad (37)$$

so that for proton-proton dipolar interactions which are not averaged out by molecular motion and $r = 2.5 \text{ \AA}$ one finds $\tau_{bg} = \tau_{\text{cross}} \approx 0.3 \times 10^{-4} \text{ s}$. Since bonding of water molecules is not completely rigid, this estimate represents just the lower limit of τ_{bg} .

The rate equations for the z -components of the proton magnetization of water molecules (M_b) bonded for

a time $\tau_b > \tau_{bg} = \tau_{\text{cross}}$ to the gel (M_g) are

$$\frac{d}{dt} M_b = -\frac{1}{T_{1b}} (M_b - M_{b\infty}) - \frac{1}{\tau_{bg}} M_b + \frac{1}{\tau_{gb}} M_g, \quad (38a)$$

$$\frac{d}{dt} M_g = -\frac{1}{T_{1g}} (M_g - M_{g\infty}) - \frac{1}{\tau_{gb}} M_g + \frac{1}{\tau_{bg}} M_b, \quad (38b)$$

where the equilibrium values $M_{g\infty}$ and $M_{b\infty}$ and exchange rates τ_{bg} and τ_{gb} are related by

$$\tau_{bg} M_{b\infty} = \tau_{gb} M_{g\infty}. \quad (39)$$

Introducing

$$m_i = (M_i - M_{i\infty})/M_{i\infty}, \quad i = b, g \quad (40)$$

this becomes:

$$\frac{d}{dt} m_b = -T_{1b}^{-1} m_b - \tau_{bg}^{-1} (m_b - m_g), \quad (41a)$$

$$\frac{d}{dt} m_g = -T_{1g}^{-1} m_g - \tau_{gb}^{-1} (m_g - m_b), \quad (41b)$$

From $M_{g\infty} \gg M_{b\infty}$ one finds $\tau_{gb}^{-1} \ll \tau_{bg}^{-1}$. One should further note that the bonded water can relax via the gel only if $T_{1g} < T_{1b}$.

Let us now investigate the case $\tau_{gb}^{-1} \ll T_{1g}^{-1}$, $T_{1b}^{-1} \ll \tau_{bg}^{-1}$. Here we get

$$\frac{d}{dt} m_b \approx -\tau_{bg}^{-1} (m_b - m_g), \quad (42a)$$

$$\frac{d}{dt} m_g = -T_{1g}^{-1} m_g \quad (42b)$$

with the solution

$$m_b = m_{g0} \frac{\tau_{bg}^{-1}}{T_g^{-1} + \tau_{bg}^{-1}} e^{-t/T_{1g}} + \left(m_{b0} - m_{g0} \frac{\tau_{bg}^{-1}}{T_g^{-1} + \tau_{bg}^{-1}} \right) e^{-t/\tau_{bg}} \quad (43a)$$

and

$$m_g = m_{g0} \exp(-t/T_{1g}). \quad (43b)$$

m_{b0} and m_{g0} are the corresponding initial values at the beginning of the cross relaxation process, which was here chosen to start at time t_0 after the preparation pulse. Since within the gel spin diffusion is fast, T_{1g} represents the spin-lattice relaxation time of the gel. In the above case (43a) we thus have a two-exponential magnetization recovery.

For $\tau_{bg}^{-1} \gg T_{1g}^{-1}$, m_b and m_g relax with the rate T_{1g}^{-1} , which is dominated by paramagnetic impurities as described above.

For $\tau_f^{-1} \ll T_{1g}^{-1}$ the relaxation of gel protons is so fast compared to the water exchange that during most of this exchange process the magnetization of gel protons is already zero. Therefore for all times $t_0 > T_{1g}$ one can use $m_{g0} \approx 0$ so that

$$m_b = m_{b0} \exp(-t/\tau_{bg}), \tag{44}$$

and the magnetization recovery becomes mono-exponential. In this case the effective spin-lattice relaxation time of water molecules bonded to the gel surface is the cross-relaxation time $\tau_{bg} \ll \tau_{gb}$ and not T_{1b} . Since this time is given by the square root of the inverse second moment of the dipolar interaction between the H_2O molecule and the gel, the spin-lattice relaxation rate should in this limit be independent of the nuclear Larmor frequency.

V. Experimental Results and Discussion

The inhomogeneous free induction decay time T_2^* in a fully hydrated OPC sample is significantly shorter than the homogeneous T_2 and is – within the limits of experimental error – independent of the magnetic field strength for frequencies below 100 MHz. This demonstrates that water molecule diffusion in internal magnetic field gradients (Chapt. III c)) is not a dominant spin-lattice relaxation mechanism.

The dependence of the water proton T_1 on the observation window [6] in the inhomogeneous free induction decay of a fully hydrated sample is shown in Figure 1. The relation [7] between the increment in the spin-lattice relaxation rate of exchangeable water and the compressive and bending strengths of a hardening cement paste is shown in Figure 2.

Whereas the water magnetization recovery in OPC and “white” cement is mono-exponential in the early stages of cement hydration, it becomes definitely non-exponential after the dormant period (Figure 3). The results cannot be consistently described by a decomposition into two exponentials or by Gaussian or power law distributions of T_1^{-1} . The data can however, be well described [2] by a stretched exponential proton magnetization recovery function (Fig. 3 b). The time evolution of the magnetization recovery exponent α is shown in Figure 4.

The time evolution of T_1 of “exchangeable” water protons ($30 \leq T_2 \leq 100 \mu s$) in C_3S , OPC and “white” cement pastes is shown in Figures 5a–c. In all three cases we see that T_1 is nearly constant in the “dor-

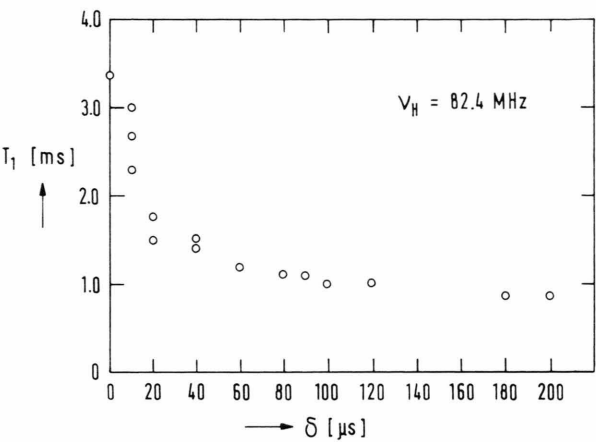


Fig. 1. The dependence of the water proton T_1 on the observation window δ in the inhomogeneous free induction decay in a white cement paste sample after 8.5 months of hydration.

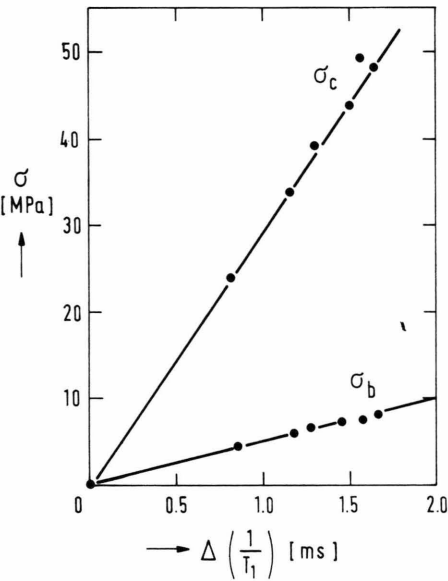


Fig. 2. Relation [7] between the increment (with respect to the dormant period) in the spin-lattice relaxation rate $\Delta(T_1^{-1})$ of “exchangeable” water and compressive (σ_c) and bending strength (σ_b) of a hardening OPC paste.

mant” period, rapidly decreases in a period when the compressive and bending elastic strength of cement starts to increase from zero (Fig. 2), and then slowly decreases with increasing hydration time. This is similar to the time evolution of α . In spite of the similarity of the T_1 versus hydration time curves in all three

above compounds, there is a marked difference in the actual magnitudes of the observed spin-lattice relaxation times.

In a C_3S paste ($w/c = 0.45$) the proton T_1 in the dormant period is as long as 580 ms (Figure 5a). At

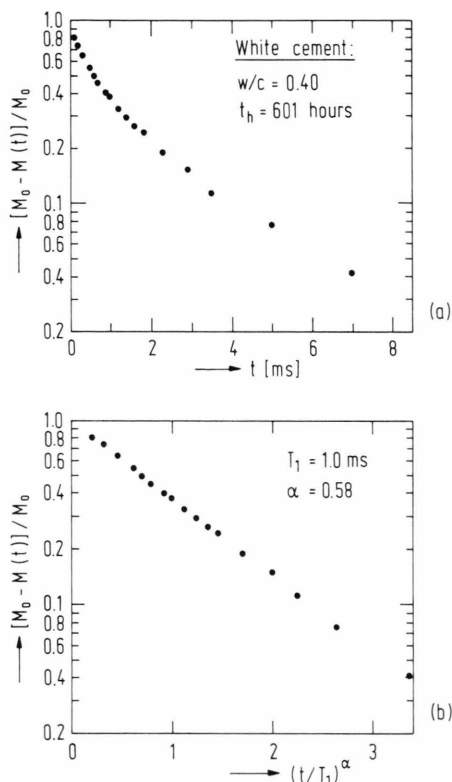


Fig. 3. Proton magnetization relaxation recovery function of exchangeable water ($30 \mu s \leq T_2 \leq 100 \mu s$) in solidifying white cement. Whereas the semilogarithmic plot of $[M(t) - M_0]/M_0$ vs. separation t between 90° pulses is clearly non-linear (a) it becomes linear (b) when $\log [M(t) - M_0]/M_0$ is plotted against $(t/T_1)^\alpha$. This demonstrates that the magnetization recovery is of the stretched exponential type rather than mono-exponential.

the end of the hydration process T_1 drops to about 200 ms. In white cement ($w/c = 0.5$) T_1 is about 50 ms in the dormant period and drops to about 1 ms at the end of the hydration process. In OPC, on the other hand, T_1 may be as short as 20 ms in the dormant period and then drops to values of the order of 1 ms or less after 28 hours.

The differences in T_1 between C_3S , white cement and OPC in the dormant period clearly show the importance of paramagnetic iron ions in determining the proton T_1 . The same is true for the difference in T_1 between C_3S and OPC at the end of the hydration process. Here the ratio between the corresponding T_1 values $[T_1(C_3S)/T_1(OPC) \approx 200]$ approximately corresponds to the ratio between the iron concentrations in the two compounds.

To understand the time development of T_1 in these systems and its relation to the compressive and bending strengths of the hardening cement paste we have to recall some structural properties of the fresh and hardened paste. When cement and water are first brought into contact, a rapid chemical reaction occurs. Within about five minutes the reaction subsides to a low level and one enters the dormant period during which the cement paste is plastic. The fraction of cement used up in the initial reaction is only about 1%, and the cement grains appear virtually unchanged. The grains are covered with insoluble reaction products which are hydrophylic. The liquid phase of the mixture is an aqueous solution of Ca^{++} , Na^+ , K^+ , OH^- and SO_4^{2-} ions with a pH in the neighbourhood of 13. At the end of the dormant period a relatively rapid chemical reaction sets in, cement gel develops and the paste loses its plasticity. After that, the chemical reactions continue at a diminished rate until all cement is consumed. The cement gel tends to fill the capillary channels of the fresh paste, thus reducing the

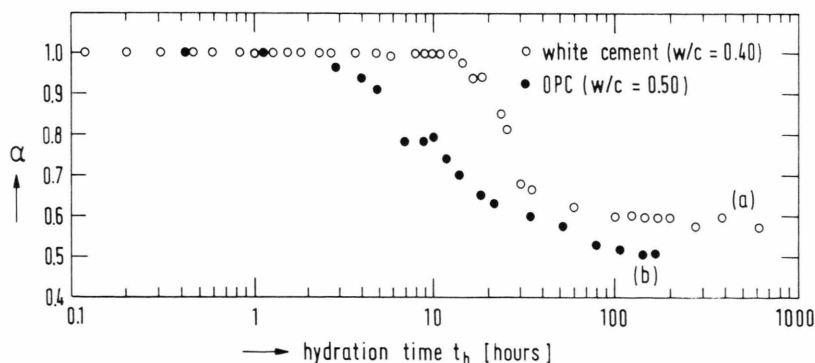


Fig. 4. Dependence of the stretched-exponential exponent α on hydration time t_h in (a) white cement and (b) OPC.

capillary size and destroying the continuity of the capillaries. Since there is no continuous capillary system anymore, the flow cannot bypass the cement gel. When the continuity of the capillary system is lost, the gel system becomes connected so that one could describe the hardening of cement in terms of a connectivity transition as described by percolation theory. The connectivity transition gives rise to the finite elastic strength of the cement paste.

The reduction in the size of the capillary cavities increases the internal surface of the cement paste, thus making it easier for the water molecules to relax via exchange with protons attached to the surface. Thus

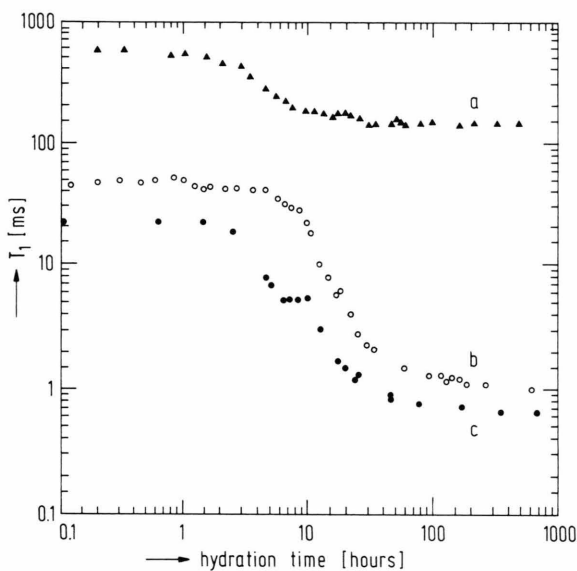


Fig. 5. Dependence of the proton spin-lattice relaxation time T_1 of "exchangeable" water on the hydration time for (a) C_3S , (b) white cement and (c) OPC.

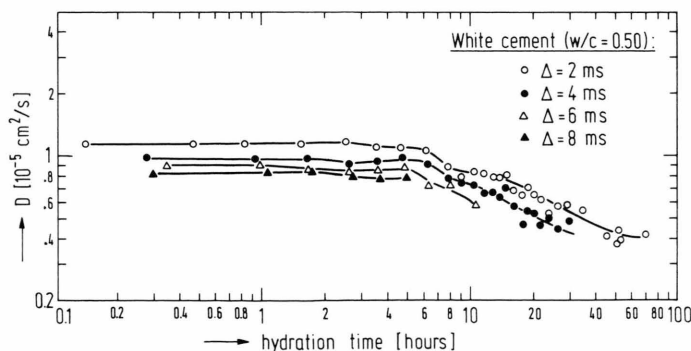


Fig. 6. Dependence of the self-diffusion coefficient D of physically adsorbed water ($T_2^* = 1$ ms) on the hydration time in a hardening white cement paste. D was determined for different diffusion time Δ by the pulsed magnetic field gradient spin-echo NMR method.

we have

$$\left(\frac{1}{T_1}\right) \approx \left(\frac{1}{T_{1b}}\right) \eta, \quad (45)$$

and the time development of T_1^{-1} reflects the time development of η . Since the elastic strength is related to the internal surface, the relation between $(1/T_1)$ and the compressive and bending strengths of the cement paste can be readily understood.

The dependence of the water self-diffusion coefficient on both the hydration time and the diffusion time for white cement is shown in Figure 6. The measurements were performed at $T = 293$ K for a water/cement ratio of 0.5 and for diffusion times $\Delta = 2, 4, 6$ and 8 ms. In contrast to the T_1 measurements, we did not study "micropore" or "interlayer" exchangeable water (where T_2^* is between 20 and 90 μ s) but rather the so called "free" or "physically adsorbed" water component (where T_2^* is of the order of a few ms). The water self-diffusion coefficient is several times smaller than in free water and decreases with increasing hydration time. This is easy to understand, as the internal surface of the cement increases with increasing hydration time thus increasing the fraction of the time a given water molecule spends bonded at the gel boundary where it is unable to diffuse freely. For fast exchange between bonded and unbonded water molecules we would thus expect

$$D = \frac{\tau_f}{\tau_f + \tau_b} D_f + \frac{\tau_b}{\tau_f + \tau_b} D_b \cong \frac{\tau_f}{\tau_f + \tau_b} D_f = (1 - \eta) D_f,$$

as $D_b \ll D_f$. Here D_f is the self-diffusion coefficient of free and D_b that of bonded water. The above model is oversimplified since it does not take into account the direct steric hindrance of the "silicon garden" in the

cement gel. That this is indeed the case is shown by the dependence of D on the diffusion time Δ . D decreases with Δ . In view of the short T_2 it was impossible to check whether the decrease of D with Δ is due to restricted diffusion in a cavity or due to diffusion in a porous medium.

It should be further noted that the root mean square displacement

$$R = \sqrt{6Dt} \quad (47)$$

of a water molecule in the time of 1 ms (i.e. the shortest T_1) is about 2 μm , thus confirming the assumption of fast exchange within a given micropore.

The temperature dependences of the homogeneous T_2 between +80 °C and –80 °C – measured with a Carr-Purcell sequence – and the inhomogeneous free induction decay time T_2^* are shown in Fig. 7 for 44.4 MHz. At all temperatures above –20 °C T_2 is longer than T_2^* , demonstrating the inhomogeneous nature of the proton signal in cement paste. Both T_2 and T_2^* decrease with decreasing temperature. The difference between T_2 and T_2^* disappears around –20 °C. This demonstrates that water freezing at or below this temperature so that the dipolar broadening is becoming larger than the inhomogeneous broadening.

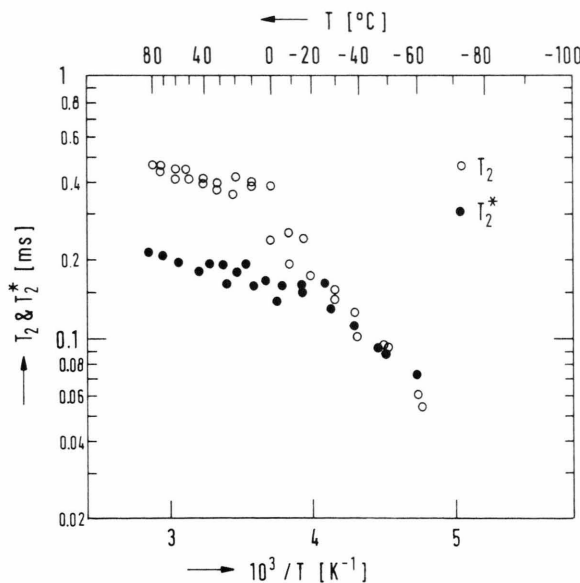


Fig. 7. Temperature dependence of the homogeneous spin-spin relaxation time T_2 and the free induction decay time T_2^* in a white cement paste ($w/c = 0.4$) after 8.5 months of hydration.

The Larmor frequency dependence of the proton T_1 of the cement gel water ($\delta = T_2 \approx 18 \mu\text{s}$) in a 4 years old sample of OPC ($w/c = 0.26$) is shown in Fig. 8 for temperatures between +80 °C and –80 °C. The data at 58.2, 46.9, and 33.3 MHz clearly show the presence of a T_1 minimum which shifts from 42 °C at 58.2 MHz to approximately 30 °C at 33.3 MHz. On the low temperature side of the T_1 minimum T_1 increases with decreasing temperature, as expected for a thermally activated processes $T_1 \propto \tau_0 \exp(E_a/kT)$ with $E_a = 0.11 \text{ eV}$. The Larmor frequency dependence of T_1 is here relatively weak, $T_1 \propto \omega_L^{-0.8}$, as expected for the case where the relaxation of the gel protons takes place via spin diffusion (23) to paramagnetic impurities. The relaxation of the water protons is then given by (15b), and the decay of the bonded water proton magnetization by (43a). In view of the roughness of the gel-water interface, the magnetization decay will in fact be given by (2) and (1) rather than (43a). The shape of the T_1 vs. $1/T$ curve cannot quantitatively described by the BPP theory [10]. This is of course expected for the case where we deal with a broad distribution of correlation times.

The temperature dependences of T_1 of exchangeable water in white cement at 30, 54.96 and 270 MHz after 80 days of hydration are shown in Figure 9. In all cases, $T_1 \propto (T_{1b})_{\text{eff}}$ decreases with increasing temperature from –80 °C till room temperature, where a flat T_1 minimum or a plateau is reached. The room temperature value of T_1 increases from 1.3 ms at 54.96 MHz to 6 ms at 270 MHz. The $\log T_1$ vs. ω_L curve (insert to Fig. 9) clearly shows the presence of two different regimes, demonstrating that more than one relaxation mechanism contributes to the proton T_1 in white cement.

The values of the rotating frame spin-lattice relaxation time $T_{1\rho}$ (Fig. 9) are – at $H_1 = 8 \text{ Gauss}$ – of the order of 0.7 ms at room temperature and show a similar T -dependence as the T_1 data. The $T_{1\rho}$ minimum is very broad and flat and extends from +80 °C to –60 °C. Only below –60 °C the limit $\omega_L \tau \ll 1$ seems to be reached and $T_{1\rho}$ starts to increase with decreasing T . In view of the observed Larmor frequency dependence of T_1 and $T_{1\rho}$ it is clear that – at least in OPC and white cement – spin-lattice relaxation is below 100 MHz after the dormant period dominated by spin diffusion to paramagnetic impurities. The fact that the T_1 minimum is extremely broad reflects the fact that we deal with a broad distribution of correlation times, as expected for space fractal system.

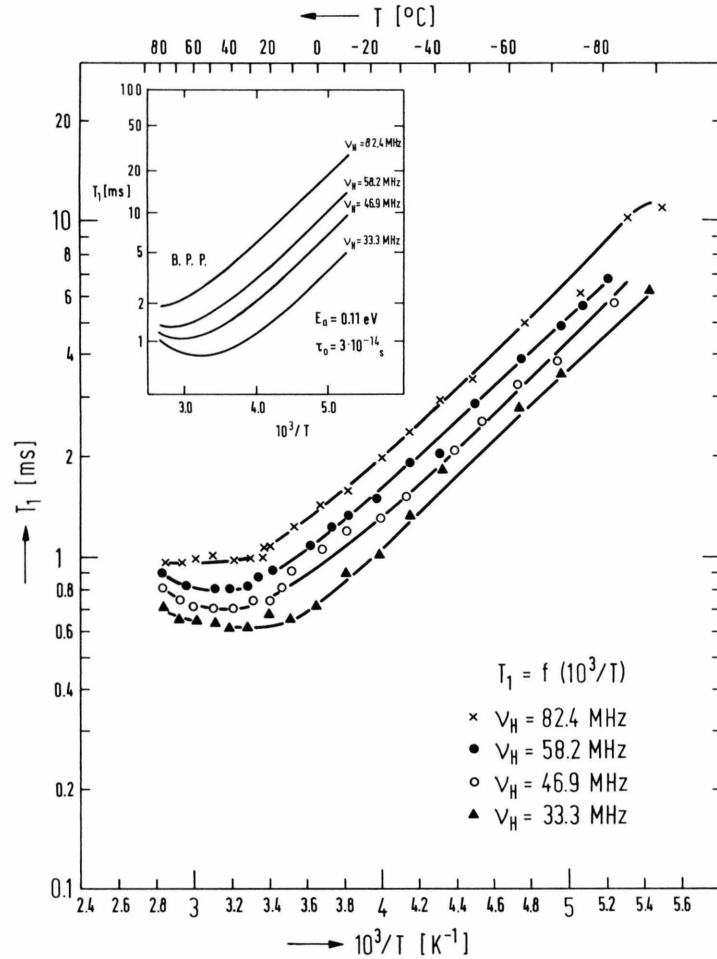


Fig. 8. Temperature dependence of the NMR spin-lattice relaxation time T_1 of gel protons in OPC at different Larmor frequencies after 4 years of hydration. The insert shows the predictions of the BPP model [10].

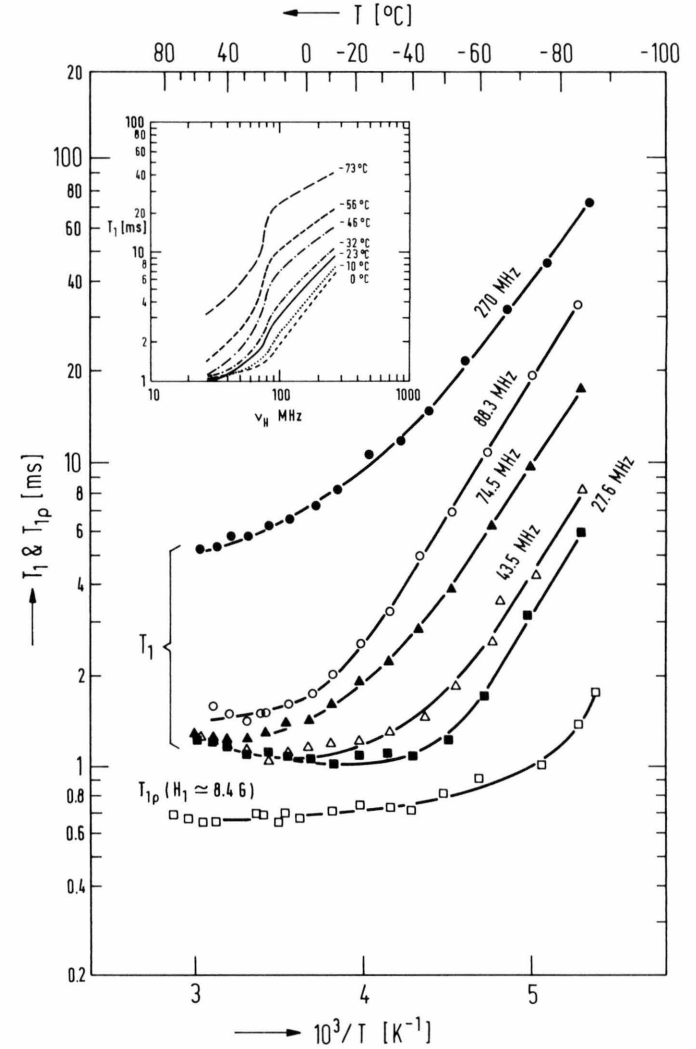


Fig. 9. Temperature dependence of the proton spin-lattice relaxation time T_1 of exchangeable water in white cement at several Larmor frequencies ν_H after 80 days of hydration. (The insert $\log T_1$ vs. ν_H clearly shows the presence of two different relaxation regimes.) The rotating frame proton spin-lattice relaxation time $T_{1\rho}$ shows a similar temperature dependence as the T_1 data. Extremely broad spin-lattice relaxation time minima indicate a broad distribution of correlation times as expected for a space fractal system.

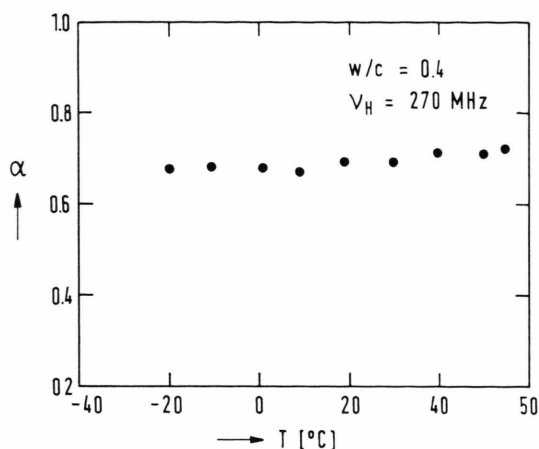


Fig. 10. Temperature dependence of the stretched exponential magnetization recovery exponent α in white cement after 18 days of hydration.

The temperature independence of the stretched exponential magnetization recovery exponent α (Fig. 10) further demonstrates that the observed non-exponentiality of the proton magnetization relaxation recovery at long hydration times is not a dynamic but rather a static effect entirely due to the size distribution and fractal geometry of the micropores.

Different models of cement hydration lead to different scaling ratios for the gel surface to volume ratio $\eta = \eta(\xi)$ and the pore size probability distribution $g(\xi)$.

There is no general theory of irreversible growth processes as yet, and in most cases one has to rely on

numerical methods. The observed "stretched exponential" form of the nuclear magnetization recovery of exchangeable water in cement pastes and the variation of the stretched exponential exponent α with hydration time can be reproduced by the percolation model where the solidification of cement is considered as a connectivity transition between a zero-dimensional network (the initial water dispersion of cement grains) and a three dimensional network in the fully hydrated cement. Within this model the stretched exponential exponent α is given by $\alpha = y/(x + y)$, where $x = D_v - D_s$ measures the difference in the volume and surface fractal dimensions D_v and D_s , respectively, and y is the exponent determining the pore size probability distribution $g(\xi)$ close to the percolation threshold [9].

For very large clusters $y = 1$ for $p < p_c$, i.e. for the percentage hydration p being below the percolation threshold p_c , whereas $y = 2/3$ for $p > p_c$ in the three dimensions [9]. Similarly x varies from 0 for very stringy clusters to $1/3$ for compact clusters [9]. The above model thus qualitatively describes the observed decrease of α from 1 in the dormant period to ≈ 0.66 at the end of the hydration process. The corresponding value for the difference in the volume and surface fractal exponents $x = D_v - D_s \approx 0.3$, in particular, agrees rather well with the surface fractal exponent $D_s = 2.7$ found by neutron scattering [4] for cement gel after 28 days of hydration.

This is of course just one of many possibilities and additional work is needed to determine the physics of the solidification of cement.

- [1] See, for instance, R. B. Williamson, *The Solidification of Portland Cement*, Progress in Materials Science, Pergamon Press, Oxford 1972, Vol. 15, p. 189. – See also: H. F. W. Taylor, *The Chemistry of Cements*, Academic Press, London 1964.
- [2] D. D. Double and A. Hellawell, *Nature*, London **261**, 486 (1976).
- [3] D. Pearson and A. J. Allen, *J. Mat. Sci.* **20**, 303 (1985).
- [4] A. J. Allen, R. C. Oberthur, D. Pearson, P. Schofield, and C. R. Wilding, *Phil. Mag. B* **56**, 263 (1987). – See also: A. J. Allen and P. Schofield, in: *Scaling Phenomena in Disordered Systems* (R. Pynn and A. Skjeltorp, eds.), p. 189. NATO ASI, B **133**, Plenum Press, New York 1985.
- [5] R. Blinc, G. Lahajnar, S. Žumer, and M. M. Pintar, to be published.
- [6] See, for instance, L. J. Schreiner, J. C. McTavish, L. Miljković, M. M. Pintar, R. Blinc, G. Lahajnar, D. Lasić, and L. W. Reeves, *J. Amer. Ceram. Soc.* **68**, 10 (1985).
- [7] L. Barbič, I. Kocuvan, J. Uršič, G. Lahajnar, R. Blinc, I. Zupančič, and M. Rožmarin, *Ciment, Betons, Platres, Chaux* **718**, 172 (1979).
- [8] R. G. Palmer, D. L. Stein, E. Abrahams, and P. W. Anderson, *Phys. Rev. Letters* **53**, 958 (1984) and references therein.
- [9] G. S. Crest and M. H. Cohen, *Ann. Israel Phys. Soc.* **5**, 187 (1983).
- [10] A. Abragam, *The Principles of Nuclear Magnetism*, Oxford University Press 1960.
- [11] J. A. Glasel and K. H. Lee, *J. Amer. Chem. Soc.* **96**, 970 (1974). – D. P. Gallegos and D. M. Smith, *J. Colloid Interface Sci.* **122**, 143 (1988).